Available Online at www.e-iph.co.uk
Indexed in Clarivate Analytics WoS, and ScienceOPEN

E-B Environment - Behaviour Proceedings Journal

ICWEP2022

https://icwep.uitm.edu.my/index.php
International Conference on Wood and Eco-Products 2022
Best Western Hotel iCity, Shah Alam, Selangor, Malaysia 15-16 Nov 2022
Organiser: Faculty of Applied Sciences, Universiti Teknologi MARA (UiTM), Shah Alam Malaysia & Research Nexus UiTM,, Office of Deputy Vice-Chancellor (Research & Innovation)

e-IPH e-International Publishing House Ltd., United Kingdom

Possible Application of Activated Palm Kernel Shell (APKS) from Palm Oil Industry as Potential Filler in Carboxylated Nitrile Butadiene Rubber (XNBR)

Siti Nur Liyana Mamauod[1*,2], Syazwani Aqilah Zainal Rashid [2], Nahrul Hayawin Zainal [3], Hanafi Ismail [4]

[1*] Center for Chemical Synthesis & Polymer Technology, Institute of Science, Universiti Teknologi MARA, 40450 Shah Alam, Selangor, Malaysia
[2] Faculty of Applied Sciences, Universiti Teknologi MARA, 40450 Shah Alam, Selangor, Malaysia
[3] Green Products Development, Biomass Technology Unit, Engineering and Processing Division, Malaysian Palm Oil Board, Malaysia
[4] School of Materials & Mineral Resources Eng., USM Eng. Campus, 14300 Nibong Tebal, Penang, Malaysia

nurliyana2219@uitm.edu.my, wanizainalrashid@gmail.com, nahrul.hayawin@mpob.my, ihanafi@usm.my
Tel: +603-55435527*:

Abstract
In this study, different APKS loadings from 0 phr to 50 phr were incorporated into the carboxylated butadiene rubber (XNBR). The average filler particle size was identified as between 1.217 to 31.944µm based on particle size analysis. The curing, crosslink density, tensile properties, and morphology values of the APKS-filled XNBR were studied. The incorporated APKS has increased the crosslink density, delta torque, cure time (t90), and decreased the swelling degree of the XNBR. The overall mechanical properties were enhanced due to the mechanical interlocking of rubber-filler phases until the optimum APKS loading which was 40 phr.

Keywords: Activated palm kernel shell, biofiller; carboxylated nitrile butadiene rubber, mechanical properties

DOI: https://doi.org/10.21834/e-bpj.v9iSI17.5452

1.0 Introduction

Malaysia is the second largest palm oil producer in the world. The palm oil production globally has increased from 15 million tons in 1995 to 66 million tons in 2017. In 2015, the palm oil industry generated 75.61 million tons of solid biomass waste. The statistic keeps increasing due to the fast growth of plantations in the palm oil industry. Biomass waste generated about 85-110 million tons in 2020 (Ong et al., 2021). The rapid oil production, palm biomass is under-utilized and unsystematically disposed of via open burning, leading to air pollution. Direct burning of biomass produces dust emissions and smoke due to incomplete combustion, which is not environmentally friendly. Many efforts have been made to address the issue by utilizing PKS as a biofiller in rubber compounding. This development of renewable bioresources in the rubber industry provides a novel alternative to dispose of agricultural wastes. Rubber-filler interaction plays a vital role in the utilization of biofiller in a rubber compound. The excellent performance of rubber products is attributed to the surface area, size, loading, surface activity, and dispersion state of the filler particles. When rubber and filler interact well, the vulcanised rubber can move stress from the rubber chains to the filler, which improves the performance of the vulcanised rubber (Abidin et al., 2020).

eISSN: 2398-4287 © 2024. The Authors. Published for AMER and cE-Bs by e-International Publishing House, Ltd., UK. This is an open-access article under the CC BY-NC-ND license (http://creativecommons.org/licenses/by-nc-nd/4.0/). Peer–review under responsibility of AMER (Association of Malaysian Environment-Behaviour Researchers) and cE-Bs (Centre for Environment-Behaviour Studies), College of Built Environment, Universiti Teknologi MARA, Malaysia.
DOI: https://doi.org/10.21834/e-bpj.v9iSI17.5452

In this study, APKS has been incorporated into XNBR to explore the potential of APKS as a biofiller. The size of the fine particles in APKS was measured by conducting a particle size analysis. Then, the APKS were incorporated into the XNBR with different loadings: 0, 5, 10, 20, 30, 40, and 50 phr. This work was conducted to study the curing characteristics, swelling properties, crosslink density, and morphology analysis of the APKS-filled XNBR. Tensile testing was carried out to study the mechanical properties of the APKS-filled XNBR. This approach promotes a bio-based economy, aligns with government regulation, and meets the 12th (Responsible Consumption and Production) and 13th (Climate Action) Sustainable Development Goals (SDGs) by producing sustainable biofiller in rubber.

2.0 Literature Review

As stated in a study of raw PKS characterization, the smooth surface of raw PKS leads to a small surface area that reduces the rubber-filler interaction. The filler must make intimate contact with the rubber chain to reinforce the filler and rubber. However, the low filler surface area has a limited contact area, reducing the potential to reinforce the rubber chain. The dirt and impurities on the raw PKS surface have caused poor interaction between the filler surface and rubber. Moreover, the low carbon content in raw PKS also contributes to the poor mechanical properties of the vulcanised rubber. Carbon content in the filler is crucial, as it can naturally form a strong interaction with the hydrocarbon chain in rubber. Thus, the high carbon content of the filler is preferred (Prajapati Naik et al., 2020). The presence of lignin, hemicellulose, and cellulose (44.0%, 21.6%, and 27.7%, respectively) reduces the filler surface activity in rubber. This fibre macromolecule has many polar functional groups, including phenolic hydroxyls, carbonyl, carboxyl, aliphatic, and phenolic hydroxyls (Aini et al., 2020). This makes it very polar. The very high filler polarity in rubber will strengthen the interaction between fillers due to strong inter- and intra-molecular interactions, thus causing agglomeration. The agglomeration in the rubber compound will initiate fracture when subjected to the strain due to the non-uniform stress transfer. The presence of both cellulose and hemicellulose will disturb the interaction between rubber and filler. These weaknesses of raw PKS can lead to poor reinforcement that lowers the mechanical properties of the vulcanised rubber.

In the past, many studies used APKS that had been chemically activated as a possible biofiller in a rubber matrix to get around the problems with raw PKS (Ban et al., 2022; Sakhiya et al., 2020). However, the chemical activation does harm the equipment because the corrosion will be intense at high temperatures. In terms of efficiency, the chemical activation is sensitive to the activation agent concentration, type of activation agent, activation temperature, and mixing intensity. A very high concentration of the activation agent can shrink the pore volume and cause the physical collapse of the carbon structure. On an industrial scale, a significant effort in the washing process is required to minimise the effects of chemical pollution on the environment (Hsiao et al., 2023).

Since no one has ever looked into adding physical APKS to a rubber matrix before, this study used the carbonisation and steam treatment processes to turn the raw PKS into something usable. The steam treatment was done to develop more pores and enlarge the existing pores produced during carbonisation, which increases the surface area of carbonised PKS, leading to better reinforcement. The carbonisation process increased the carbon content in PKS from 46.93 wt% to 84.77 wt%. Meanwhile, oxygen and hydrogen decreased due to dehydration during the process. Therefore, the carbon content can form a strong interaction with the hydrocarbon chain of the rubber (Christopher et al., 2021). The lignin that contains polar functional groups would extremely decrease after carbonisation due to the dehydration and deoxygenation reactions. The APKS's degraded polar functional groups made the filler surface more active, which helped the rubber and filler stick together and stopped them from sticking together because of the weak interaction between the two. This made the filler more evenly distributed in the rubber matrix. The dirt and impurities were also degraded during the carbonisation process. This degradation will enhance the interaction between rubber and filler, reinforcing vulcanised rubber better (Stephanie et al., 2021).

3.0 Methodology

3.1 Materials

The APKS in this study were supplied by the Malaysian Palm Oil Board (MPOB). Airelastic Sdn Bhd supplied MBTS, DPG, TMQ, and TMTD, and ARAS BAKTI Ventures provided the XNBR. The Faculty of Applied Science at Universiti Teknologi Mara (UiTM) provided equipment for processing oil, stearic acid, zinc oxide, and sulfur.

3.2 Preparation of fine particles of activated palm kernel shell (APKS)

The APKS was supplied in large particle sizes and then ground by using a crusher to obtain a finer particle size. Next, the crushed APKS was pulverised into smaller particles, which were then sieved by using a vibratory sieve shaker (Retsch AS 20 Germany) with 240 mesh. The fine APKS particle size was identified through the particle size analysis.

3.3 Preparation of APKS-filled XNBR compound

The compounding ingredients were mixed based on the formulation, as shown in Table 1, by using a two-roll mill (2 OSAKA 18). Before adding other additives to the XNBR, the XNBR was masticated to lower the viscosity and soften the rubber. Then, the ingredients with loadings, as shown in Table 1, were incorporated during the mixing process.

Table 1. The recipe for APKS-filled XNBR compound

Ingredients (phr)	Compounding No.						
	1	2	3	4	5	6	7
XNBR	100	100	100	100	100	100	100
APKS	0.0	5.0	10.0	20.0	30.0	40.0	50.0
Activator	5.0	5.0	5.0	5.0	5.0	5.0	5.0
Antioxidant	0.8	0.8	0.8	0.8	0.8	0.8	0.8
Accelerator	3.7	3.7	3.7	3.7	3.7	3.7	3.7
Sulphur	1.3	1.3	1.3	1.3	1.3	1.3	1.3
Processing oil	5.0	5.0	5.0	5.0	5.0	5.0	5.0

3.4 Characterization

The particle size analysis was carried out to identify the average APKS particle size and size distribution by using Fritsch Laser Particle Sizer Wet Dispersing. The curing behaviour was determined according to ASTM 2048 by using the rubber rheometer ZME 1005A. The sample with a weight of 7–10 g was placed on the rheometer's die. The optimum cure time (t_{90}), scorch time (t_2), minimum torque (M_L), maximum torque (M_H), and delta torque (M) were obtained. The cure rate index (CRI) was then calculated according to Equation (1).

$$CRI=\frac{100}{(t90-ts2)} \quad (1)$$

The swelling measurement was carried out to investigate the solvent resistance of the vulcanised rubber based on ASTM 471. Seven samples containing different loadings of APKS in XNBR with a size of $(1 \times 1)cm^2$were immersed in a toluene solution until saturation was reached. The samples were weighed until they reached a constant weight, and then the samples were dried in an oven at 70°C. The dried samples were weighed to obtain their final weight. This analysis was performedree times. The swelling index (SI) was calculated based on ASTM 471 using Equation (2).

$$\text{Swelling index (SI) (\%)} =\frac{(final\ weight-initial\ weight)}{initial\ weight} \quad (2)$$

The crosslink density was calculated by using the Flory-Rehner equation based on ASTM D6814, as given in Equation (3). Vr is the rubber volume fraction in the swollen gel, X is the rubber-solvent interaction, which is 0.487, and $(x)_{phy}$ is the crosslink density.

$$-\ln(1-V_r)-V_r -XV_r =2\ \rho(x)_{phy}V_r^{1/3} \quad (3)$$

According to ASTM D412, at room temperature, the Instron 33366 machine performed a tensile test. The samples were prepared by cutting them into flat sheets of dumbbells. The overall length of the specimen is 155 mm, and the gauge length is 25mm. The speed of testing was 500 mm/min. Tensile strength, elongation at break, and M300 were obtained. The reinforcement index (RI) was calculated based on (4).

$$\text{Reinforcing index (\%)} = M300/M100 \quad (4)$$

SEM analysis was conducted based on ASTM D8363. The tensile-ruptured surfaces of APKS-filled XNBR were used throughout the morphology study. The tensile failure surface of APKS-filled XNBR was used throughout the study. After the tensile test, the broken samples are put through SEM analysis to find out how the filler is distributed in the XNBR matrix. The level of distribution affects how well the filler and rubber interact. The samples were coated with 20–30 nm of gold to surface charge and promote secondary electron emission to provide a homogeneous surface for imagining and analysis.

4.0 Results and Discussion

4.1 Properties of an Activated kernel shell

Table 2. The percentage volume of particle size of the APKS sample

Particle size (µm)	Percentage volume (%)::
0.05	1
2	23.327
5	26.639
10	18.308
20	5.306
30	24.931
32	2.5

The filler particle size is a crucial factor influencing the filler's mechanical performance in vulcanised rubber. Fine particle size provides a large filler surface contact area, which promotes better mechanical properties of the rubber (Ekwueme et al., 2016). The particle size analysis was carried out to identify the range of the particle size. The range of the average particle size obtained was between 1.217

and 31.944 µm. Table 2 illustrates the volume percentage of the APKS particle size. The sample's volume percentage was 26.639% for 5 m APKS, 24.931% for 30 m, 23.327% for 2 m, and 18.308% for 10 m, respectively. These particle sizes were finer than those obtained in previous studies by Ekwueme et al. (2015), Daud et al. (2016), Molomo et al. (2020), and Hasana et al. (2021). The finer filler particle size is preferred to reinforce by having a large contact area with the rubber matrix. On the other hand, larger filler particle sizes may localise stress during the applied force, leading to early rupture (Paleri et al., 2021).

4.2 Cure characteristic of XNBR filled APKS

Table 3 shows the cure characteristic results of the vulcanized APKS filled XNBR. The t2 and ML showed no significant changes as the APKS loadings were incorporated into the compound. On the other hand, the t90 decreased significantly when the APKS loading increased; this is due to the effect of the alkaline pH of ashes on the APKS surface, which slows the t90. The MH increased when the APKS loading increased, which this result correlates to the increasing viscosity due to the formation of filler, rubber, and rubber-filler networks (Amin et al., 2020). The △M roughly indicates the crosslink of the vulcanized rubber that is in line with the increasing crosslink density. The △M increased until the APKS loading reached 40 phr. At 50 phr, the △M decreases, which might occur due to the agglomeration of APKS particles (Greenough et al., 2021).

Table 3. Cure Characteristic of XNBR Filled APKS

APKS Loading (phr)	M_L	M_H	△M	t_{90}	t_2	CRI
0	2.747	14.583	11.836	8.41	3.11	18.868
5	2.666	14.512	11.846	8.48	3.07	18.484
10	1.848	16.793	14.956	9.08	3.02	16.501
20	2.027	15.397	13.370	12.10	3.03	11.025
30	2.013	15.857	13.844	13.00	2.52	9.541
40	2.294	19.650	17.356	16.43	1.08	6.988
50	2.850	17.187	14.30	20.05	2.30	5.942

4.3 Swelling properties and crosslink density

The swelling index was calculated to study the ability of the vulcanised rubber to prevent the solvent from penetrating the rubber chain crosslink. The swelling index decreased when the APKS was incorporated into the XNBR due to the excellent rubber-filler interaction. As seen in Fig. 1, the unfilled XNBR resulted in the highest swelling index of 160.72%, which indicates poor resistance towards the solvent due to the low crosslink density since the solvent can easily penetrate the rubber chain with a low crosslink density. Hence, the swelling index is inversely proportional to the crosslink density. The unfilled XNBR showed the lowest crosslink density of 8.90%. Then, the swelling index decreased to 147.85%, 145.45%, 137.77%, 134.93%, 127.97%, and 117.21% with the presence of 5, 20, 30, 40, and 50 phr of the APKS loading, respectively, corresponding to the increasing crosslink density of 8.90%, 29.27%, 32.20%, 43.34%, 50.33%, and 84.33% at 5, 10, 20, 30, 40, and 50 phr of the APKS loading, respectively.

Therefore, the APKS loading increased the crosslink density and reduced the swelling index (Mehdi et al., 2022). The excellent interaction between XNBR and APKS promoted the crosslink density and immobilised the rubber chain, which improved the swelling resistance by reducing solvent penetration into the rubber chains. The irregularity and porous structure of the APKS enhanced the physisorption, thus improving the solvent resistance of the APKS-filled XNBR (Fatin et al., 2015).

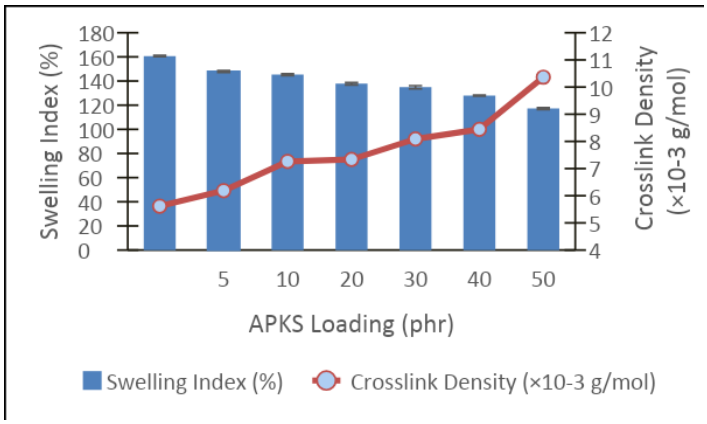

Fig. 1: The swelling index and crosslink density of the APKS-filled XNBR

4.4 Tensile properties

As can be seen from Fig. 2 (a), the tensile strength increased as the APKS loading increased until 40 phr. The unfilled XNBR resulted in the lowest tensile strength at` 7.24 MPa. There was a direct stress transfer from one rubber chain to another during the applied force, which resulted in an early rupture in the unfilled XNBR. The presence of the APKS improved the tensile strength from 3.83% to 7.73%, 12.43%, 14.91%, and 19.06% with 5, 10, 20, 30, and 40 phr of loading, respectively. When the porous APKS was mixed with the XNBR matrix, the rubber chain went through the filler pores. This made it hard for the rubber chain to move because the filler pores fit together

well (Daud et al., 2016). The adsorption of rubber molecules on the porous APKS surface has potentially induced strain-independent contributions in the rubber matrix. Thus, these interactions resulted in efficient stress transfer from rubber chains to the APKS particles (Ban et al., 2022). The mechanical interlocking between APKS and XNBR also promoted the crosslink density, as revealed in Fig. 1. The crosslink density has led to a stress-relieving mechanism when the crosslink breaks and slips under the localised share of the neighbouring chains. More chain segments were introduced as the crosslink density increased. Short- and long-chain segments are distributed randomly in the network. The shortest chain broke early, and the applied stress was transferred to the adjacent chains. Then, a minimal number of crosslinks transferred and supported high stress until a complete rupture finally occurred. The tensile strength was improved by increasing the crosslink density until it reached its optimum value, which is at 40 phr APKS loading. At this state, the viscous flow was no longer feasible, and a complete network was formed, which provided the sufficient number of chain segments needed for a maximum amount of crystallisation during straining. At this optimum filler loading, appreciable molecular orientation occurred over the region during the applied tensile force, and the degree of crystallisation increased, which further improved the tensile strength. The crystallites have many chains that are aligned tightly together to provide reinforcement. When the XNBR is filled with the optimum APKS loading, the applied stress is transferred to the crystals that are made up of a lump of chains, which is similar to the condition when hundreds of chains are knitted closely together when the stress is transferred (Raju et al., 2021). However, at 50 phr APKS loading, the tensile strength was reduced to 16.24%. The interaction between fillers became strong and tended to form filler agglomeration, which reduced the adhesion of the rubber to the filler surface. This has resulted in the reduced efficiency of the stress transfer from the rubber matrix to filler particles (Raju et al., 2021). The incorporation of the APKS filler reduced the elongation at break of the vulcanised rubber as a result of the immobilisation of the rubber chain due to the rubber attachment on the filler surface. This immobilisation phenomenon is known as the glassy rubber shell, which inhibits the elastic behaviour of the rubber and acts as a rigid body. The decreasing mobility of the rubber chain causes the early rupture of the sample (Raju et al., 2021). The unfilled XNBR indicated the highest elongation at break value, i.e., 1044.33%. This value then decreased with the incorporation of the APKS into the XNBR. Elongation at break value of the vulcanised rubber decreased to 55.91%, 57.54%, 59.91%, 64.91%, 69.44%, and 60.35% at the APKS loading of 5, 10, 20, 30, 40, and 50 phr, respectively.

The incorporation of the APKS into the vulcanised XNBR significantly increased the M300 and reinforcement index. Fig. 2(b) shows that the reinforcement index increased when the APKS loading was incorporated into the compound. The unfilled XNBR indicated the lowest reinforcement index, i.e., 2.3471. The result increased to 11.25%, 18.41%, 27.92%, 22.905%, and 32.22% with 5, 10, 20, 30, and 40 phr of the APKS loading, respectively. The irregular shape and rough surface of the APKS enhanced the mechanical interlocking between filler and rubber (Daud et al., 2016). As the APKS loading went from 40 phr to 50 phr, the reinforcement index went down. This was because the fillers had strong interactions with each other, which made it harder for the rubber chain to stick to the filler surface.

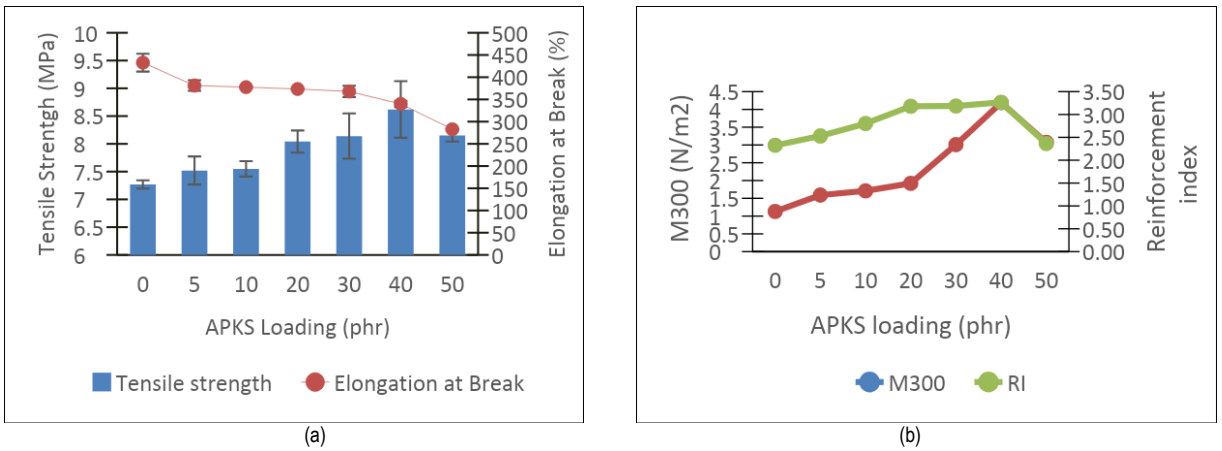

(a) (b)

Fig. 2. (a) Tensile strength and elongation at break of APKS-filled XNBR; (b) reinforcement index and M300 of APKS-filled XNBR

4.5 Morphology analysis

Fig. 3 (a) shows the surface of the ruptured tensile sample without filler. The smooth surface indicated a low resistance to tensile force. The stress was transferred directly to the adjacent rubber chain with the applied force, resulting in an early rupture. Fig. 3 (b) is the ruptured tensile sample with an optimum APKS loading of 40 phr. The compounding ingredients distributed uniformly show excellent interaction between XNBR and APKS particles. Many filler breakages indicate an efficient stress transfer from the rubber chain to the filler. The APKS particles are fully attached to the XNBR matrix,and there is no filler detachment. It is easy for the APKS particles to stick to the XNBR matrix because the fillers break apart when the tensile force is applied (Somseemee et al., 2021). Meanwhile, Fig. 3 (c) displays the above optimum APKSloading at 50 phr of the ruptured tensile surface Fillerer agglomeration is present due to strong surface energy between fillers that overcomes the interaction between rubber and filler (Raju et al., 2021). HeBecause of this, a lot of fillers have come loose from the XNBR matrix because the rubber and filler do not interact well because of the low energy transfer efficiency when tensile force is applied. When fillers come loose, they leave a space or gap between the APKS particle and the XNBR matrix because they do not fit together well mechanically (Lay et al., 2020). At 50 phr of APKS loading, the agglomeration of filler particles localises the stress during applied force and has a low resistance to tensile force, which results in the APKS being detached from the XNBR matrix.

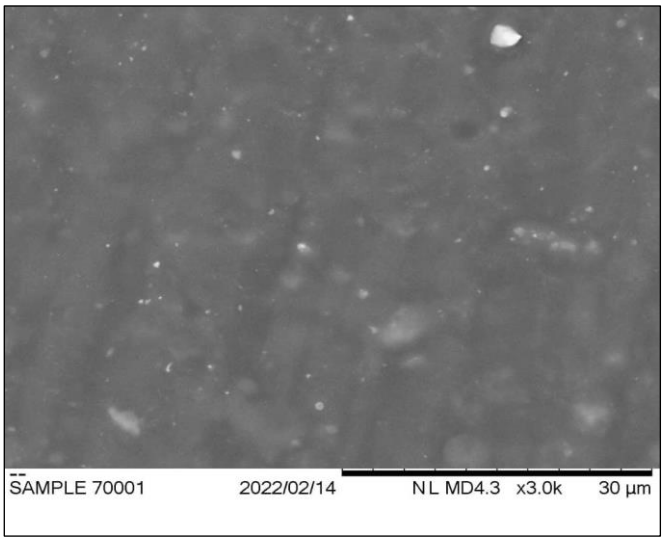

(a)

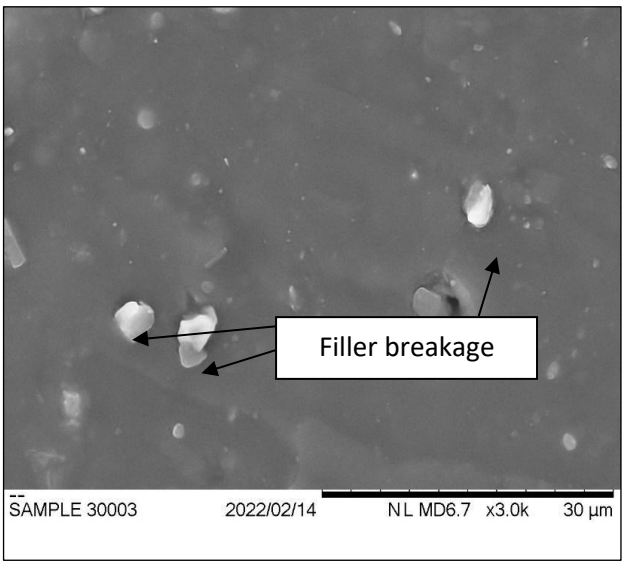

(b)

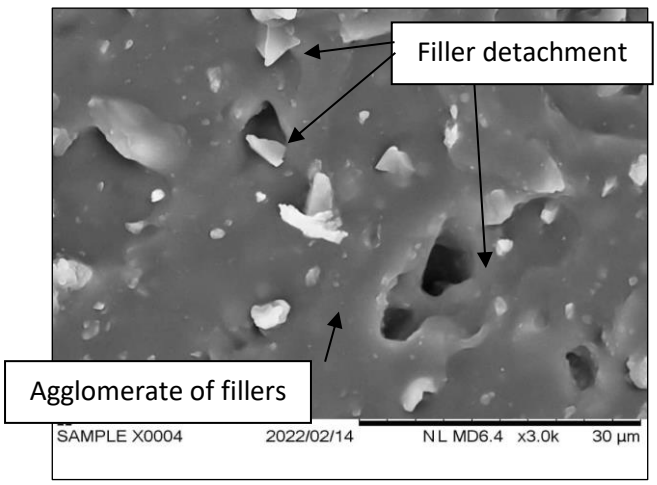

(c)

Fig. 3. SEM image of rubber composite (a) without APKS; (b) 40 phr of APKS-filled XNBR; (c) 50 phr of APKS-filled XNBR with 3000 magnification.

5.0 Conclusion and Recommendations

The characterization of the APKS has resulted in a non-homogeneous distribution of the APKS particle size. The incorporation of the APKS reduced the curing properties of the XNBR. As the optimum loading reached 40 phr, APKS improved the tensile properties of XNBR. It also increased the crosslink density, which leads to better performance of the vulcanised rubber, and it improved the swelling properties. However, some improvements can be carried out to achieve better performance in vulcanised. Further work can study the hybridization of APKS with other types of filler and incorporate nano-sized APKS, which could enhance the reinforcement in terms of crosslink density and rubber-filler interaction that result in a synergistic effect on vulcanised rubber. In a further study, a few tests or analyses, such as Raman spectroscopy and approximate and ultimate analysis, could be added to increase the finding of properties of filler that contribute to the reinforcement in the vulcanised.

Acknowledgements

It is a pleasure to see the university's provision of 'Geran Insentif Penyeliaan (GIP) 600-RMC/GIP5/3(156/2021) as the funding support to complete this study and 'Penerbitan Yuran Prosiding Berindeks' (PYPB) for providing fund support for the conference fee.

Paper Contribution to Related Field of Study

The expanding food industry contributes to the high demand for palm oil products. Consequently, increase palm oil waste. Thus, this study contributes to an environmentally friendly approach to managing palm oil waste and utilising biomass in the rubber industry.

References

Abidin, Z. Z., Mamauod, S. N. L., Sarkawi, S. S., & Saimi, N. S. B. (2020). Influence of Filler System on the Cure Characteristics and Mechanical Properties of Butyl Reclaimed Rubber. Bioresources, 5, 6045-6060.

Aini, N. A. M., Othman, N., Hussin, M. H., Sahakaro, K., & Hayeemasae, N. (2020). Lignin as Alternative Reinforcing Filler in the Rubber Industry: A Review. Frontiers in Materials.
Amin, S., Bachmann, P. T., & Yong, S. K. (2020). Oxidised Biochar from Palm Kernel Shell for Eco-friendly Pollution Management. Scientific Research Journal, 17, 44-60.

Ban, S.-E., Lee, E.-J., Lim, D.-J., Kim, I.-S., & Lee, J.-W. (2022). Evaluation Of Sulfuric Acid-Pretreated Biomass-Derived Biochar Characteristics And Its Diazinon Adsorption Mechanism. Bioresource Technology.

Christopher, G. Robertson, Ned J, & Hardman. (2021). Nature of Carbon Black Reinforcement of Rubber: Perspective on the Original Polymer Nanocomposite. Polymers

Fatin, M. H., Noriman, N. Z., Husin, K., Salihin, M. Z., Munirah, N. R., Ismail, H., Bakri, A. M. M. A., & Sam, S. T. (2015). Cure Characteristics and Physical Properties of Imperata cylindrica Activated Carbon Filled SMR L Compounding. Scientific.Net, 44-48.

Greenough, S., Dumont, M.-J. e., & Prasher, S. (2021). The Physicochemical Properties Of Biochar And Its Applicability As A Filler In Rubber Composites: A Review. Elservier.

Hsiao, Shivam Gupta, Chi-Young Lee, & Tai, N.-H. (2023). Effects of Physical and Chemical Activations on the Performance of Biochar Applied in Supercapacitors. Applied Surface Science

L.Ekwueme, O.Ogbobe, & O.G.Tenebe. (2016). Utilization Of Carbonized Palm Kernel Shell As Filler In Natural Rubber Composite. 1(1), 1-8.

Lay, M., Rusli, A., Abdullah, M. K., a, Z. A. A. H., & Shuib, R. K. (2020). Converting Dead Leaf Biomass Into Activated Carbon As A Potential Replacement For Carbon Black Filler In Rubber Composites. Elservier.

Mehdi, Barikani, & Mehburn. (2022). Determination of Crosslink Density by Swelling in the Castable Polyurethane Elastomer Based on 1/4 - Cyclohexane Diisocyanate and Para-phenylene Diisocyanate. Iranian Journal of Polymer Science & Technology, 1(1).

Ong, E. S., Rabbani, A. H., Habashy, M. M., Abdeldayem, O. M., Al-Sakkari, E. G., & Rene, E. R. (2021). Palm Oil Industrial Wastes As A Promising Feedstock For Biohydrogen Production: A Comprehensive Review Environmental Pollution.

Prajapati Naik, Smitirupa Pradhan, P. Sahoo, & Acharya., S. K. (2020). Effect of Filler Loading on Mechanical Properties of Natural Carbon Black Reinforced Polymer Composites. Materials Today: Proceedings.

Paleri, D. M., Rodriguez-Uribe, A., Misra, M., & Mohanty, A. K. (2021). Preparation And Characterization Of Eco-Friendly Hybrid Biocomposites From Natural Rubber, Biocarbon, And Carbon Black. eXPRESS Polymer Letters, 15, 236–249.

Raju, G., Khalid, M., Shaban, M. M., & Azahari, B. (2021). Preparation and Characterization of Eco-Friendly Spent Coffee/ENR50 Biocomposite in Comparison to Carbon Black. Polymer, 13.

Sakhiya, A. K., Anand, A., & Kaushal, P. (2020). Production, Activation, And Applications Of Biochar In Recent Times. Springer Science. https://doi.org/https://doi.org/10.1007/s42773-020-00047-1

Stephanie, Greenough, Marie-Josée Dumont, & Prasher, S. (2021). The Physicochemical Properties of Biochar and Its Applicability as a Filler in Rubber Composites: A Review. Materials Today Communications

Somseemee, O., Pongdhorn, Sae-Oui, & Siriwonga, C. (2021). Reinforcement Of Surface-Modified Cellulose Nanofibrils Extracted From Napier Grass Stem In Natural Rubber Composites. Elservier, 171.